JOURNAL OF PROPULSION AND POWER
Vol. 20, No. 1, January–February 2004

Characteristics of Sprays Formed by Impingement of a Pair of Liquid Jets

K. Ramamurthi,* K. Nandakumar,† and R. K. Patnaik†
Liquid Propulsion Systems Center, Trivandrum 695 547, India

The characteristic frequencies and droplet sizes in sprays formed by a pair of impinging liquid jets were experimentally determined over a wide range of Reynolds numbers. Detached, attached, and cavitated jets were used in the study. The dominant frequencies in the spray were seen to originate from the individual jets and not from the aerodynamic instability of the liquid sheet formed by the impingement. Attached flow in the nozzle led to the presence of higher frequencies in the spray. The shape of the spray was shown to transit from a diffused elliptic-shaped wavy mode to an intense conical turbulent mode when the flow through the nozzle cavitated. The inception of cavitated flow also modified the trend of the variations of droplet sizes in the spray due to changes in Reynolds number. A bimodal distribution of droplet sizes from impact and aerodynamic disintegration, obtained at the smaller values of Reynolds number, changed to an unimodal distribution from impact disintegration at larger values of Reynolds number.

Nomenclature

A	=	cross-sectional area
Cd	=	discharge coefficient
D	=	droplet diameter
d	=	nozzle diameter
l	=	length of nozzle/feedline
p	=	pressure
Q	=	volumetric flow rate
R	=	radius of jet
Re	=	Reynolds number defined by Eq. (1)
S	=	density ratio between gas and liquid
t	=	thickness of liquid sheet
V	=	velocity
We	=	Weber number defined by Eq. (6)
β	=	conservation parameter defined by Eq. (5)
Δp	=	pressure drop in nozzle
θ	=	half impingement angle of jet
μ	=	viscosity
ρ	=	density
σ	=	cavitation parameter defined by Eq. (3)
σ_l	=	surface tension coefficient
τ	=	time
Ω	=	transfer function defined by Eq. (14)
ω	=	circular frequency

Subscripts

a	=	ambient pressure
ind	=	inductive pressure drop
u	=	upper bound of frequencies
v	=	vapor pressure of water
0	=	steady state
32	=	Sauter mean

Superscript

$'$	=	perturbed quantity

Received 5 September 2002; revision received 22 May 2003; accepted for publication 7 July 2003.

*Deputy Director, Associate Fellow AIAA.
†Engineer, Propulsion Research and Studies Group.

Introduction

SPRAYS formed by impinging liquid jets have been extensively investigated over the last 50 years. The motivation for the large number of studies is based on the good mixing and atomization achievable in the impinging jet sprays and the flexibility to vary the degree of atomization and mixing. The early studies concentrated on the shape of the spray and the size of droplets formed in the spray. An elliptic liquid sheet was seen to be formed in a plane at right angles to the plane containing the axes of the jets when the diameter and momentum of the two impinging jets were equal.[1] Disturbances from the agitated zone of impact and the subsequent growth of these disturbances, either due to the inherent instability of a laterally expanding liquid sheet or from the aerodynamically induced Kelvin–Helmholtz instability, brings about the disintegration of the liquid sheet to droplets (see Ref. 1).

A physical model of reflective, merged, and transmittive atomization was used by Ashgriz et al.[2] to determine the mixing in the sprays. The degree of mixing was determined using Rupe's mixing correlation parameter, which relates the local and global values of the constituents of two jets in the spray. Both the reflective atomization, wherein the individual jets bounce off each other, and the transmittive mode for which the jets cross each other were shown to give poor mixing.

The unsteadiness in the individual jets was postulated by Anderson et al.[3] to govern the frequency of disturbances in the spray. The influence of the dynamic characteristics of the individual jets on the spray behavior, however, has not been adequately investigated. Ryan et al.[4] showed the breakup of the liquid sheet formed by the impinging jets to change significantly when the jet becomes turbulent. The flow disturbances in the jets are strongly influenced by the geometry of the injection nozzle and the Reynolds number, and these would affect the spray formed by the impingement.

The injection nozzles used in most applications have a sharp-edged entry. A nozzle is said to have sharp-edged entry when the entry radius is less than about 0.14 times the diameter of the orifice.[5] A liquid, on entering the sharp edge gets separated to form a vena contracta, as shown in Fig. 1a. The separated flow reattaches to the nozzle wall when the length of the nozzle exceeds its diameter. This is schematically shown in Fig. 1a. The static pressure at the vena contracts is lower considering the higher flow velocities due to the constriction. When the flow velocities and the backpressure are such that the static pressure at the contraction is about the vapor pressure of the liquid, nucleation of vapor bubbles takes place, resulting in cavitation. Cavitation is inherently unsteady due to implosion of the vapor bubbles in the downstream regions of higher static pressure and its interaction with the nucleation of vapor bubbles at vena contracta.

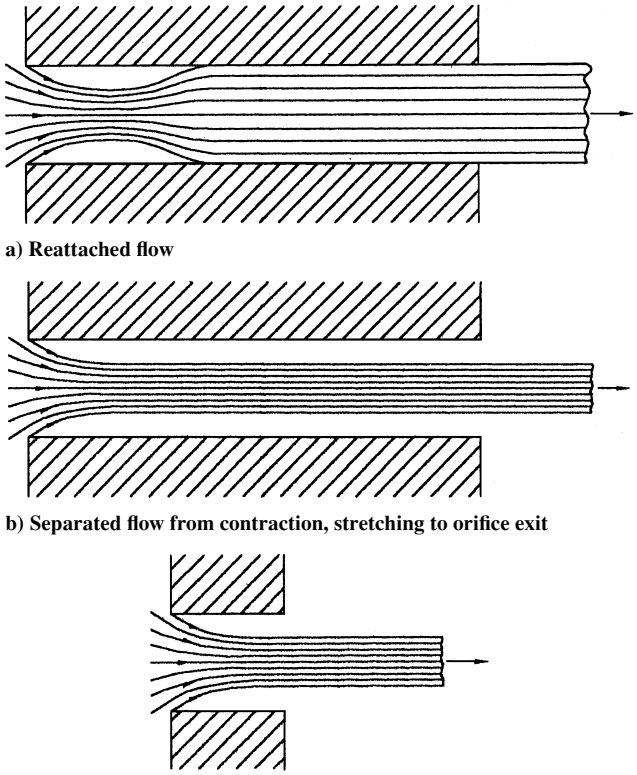

a) Reattached flow

b) Separated flow from contraction, stretching to orifice exit

c) Detached flow

Fig. 1 Schematic of attached and detached jets.

The disturbances associated with reattachment of the initially separated flow to the nozzle wall and the disturbances from cavitation have been demonstrated to promote atomization in single cylindrical jets.[6] However, their role in influencing the dynamics of the spray formed after impingement is far from being understood. Nurick[5] found that mixing within a spray, obtained by using cavitated jets, is poorer than with noncavitated jets. The atomization, being dependent on the intensification of disturbances over the liquid sheet, would be expected to improve when jet disturbances are higher. The frequencies of the disturbances would influence the droplet sizes with higher frequencies leading to smaller ligaments in the spray and, hence, smaller droplets. The early investigations of Heidmann et al.[7] gave frequencies of wave motion in the liquid sheets, formed by impingement, to be between 1000 and 3000 Hz. These are in the range of frequencies from cavitation of 2000–4000 Hz measured by Karasawa et al.[8] in sharp-edged nozzles of length-to-diameter ratio of 6.25 and 9.4. The investigations of Henry and Colocotte[9] suggest the characteristic frequencies from cavitation could be much lower because the cavitated bubbles are convected at low velocities.

The observations of Heidmann[7] of wave frequencies in the impinging spray to increase with increase of jet velocity matches with the theoretical trends obtained for aerodynamic disintegration. However, the measured frequencies are smaller than those theoretically calculated. Anderson et al.[3] and Ryan et al.[4] measured lower frequencies between 400 and 1200 Hz from high-speed movies of the impinging jets. The frequencies were seen to be reasonably independent of the jet velocity, unlike in the measurements of Heidmann et al.[7] Anderson et al.[3] suggest that these characteristic frequencies could correspond to the frequencies inherent in the individual jets before the impingement. Dombrowsky and Hooper[10] determined a significant influence of the velocity profile of individual jets on the wave motion. The characteristics of the spray would depend on whether the jets issuing from nozzles are separated, attached, or cavitated. The present study addresses the dynamics of the sprays formed by a pair of liquid jets under separated, attached, and cavitated flow conditions.

When the pressure drop across the injection nozzle is increased to much higher levels than those at which cavitated flow gets initiated, the vena contracta extends over the entire length of the orifice. The flow is then separated from the walls as shown in Fig 1b. This flow is termed as being supercavitated,[11] and the condition has also been referred to as hydraulic flip.[12] The pressure drop, or equivalently, the nozzle flow Reynolds number, at which the flip to supercavitated flow occurs, increases with an increase of the length-to-diameter ratio of the nozzle. Supercavitated jets are not subjected to the wall-induced disturbances. They are similar to the detached jet obtained in nozzles of short length-to-diameter ratio, as shown in Fig. 1c.

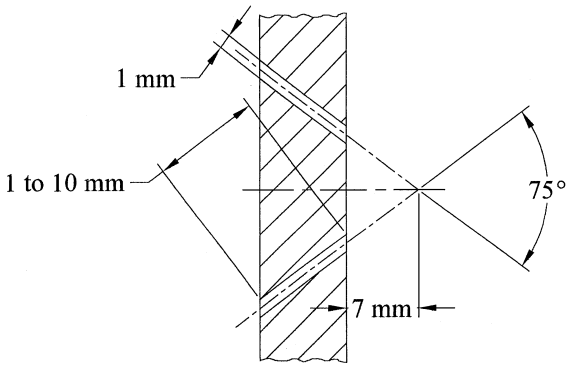

Fig. 2 Configuration of impinging injector.

The characteristic frequencies and size of droplets in the spray formed from a pair of wall-separated jets, jets attached to nozzle wall, cavitated jets, and supercavitated jets are experimentally investigated in the paper. The different regimes of the jet are obtained at different Reynolds number using sharp-edged nozzles of varying length-to-diameter ratios.

Experiments

Injectors

Doublet impinging injectors with straight cylindrical nozzles of 1 mm diameter were used for the experiments. Figure 2 shows the injector configuration. The impingement angle of the jets is 75 deg, and the distance of the impingement point from the nozzle is 7 mm. The length of the cylindrical nozzle was varied between 1 and 10 mm to give the nozzle length-to-diameter ratios between 1 and 10. The 1-mm-diam holes were drilled in aluminium blocks using a jig-boring machine. The entry to the nozzle was maintained to be sharp edged and inspected to be free of burrs.

Separated, attached, and cavitated flows were generated in the different nozzles, and the spray formed by impingement of these different types of jets was studied. The nozzle of length-to-diameter ratio of unity gave separated flow over a wide range of Reynolds number. Nozzles of length-to-diameter ratio of 2.3 and 3.3 gave attached flow at the lower range of Reynolds number and a cavitated flow followed by supercavitated separated flow at higher values of Reynolds number. The causatives and regimes of the different flows have been investigated earlier.[13,14] The nozzle of length-to-diameter ratio of 10 gave attached flow for both cavitated and noncavitated flow conditions.

Experimental Setup and Measurements

Figure 3 gives a schematic of the test setup and the measurements. Fresh tap water, after demineralizing, was stored in a run tank of 200-liter capacity and supplied to the injector through a feedline of 6 mm diameter. The injector was mounted in a cylindrical manifold 25 mm in diameter and 60 mm in length, as shown. A needle valve was provided 1.5-m upstream of the nozzle as shown.

Water in the run tank was pressurized to 1.5 MPa and discharged into the ambient atmosphere through the nozzle. The flow rate of water was determined by collecting the discharge over a few minutes in a measuring jar. The jet Reynolds number was determined from the average flow rate Q using the nozzle diameter d of 1 mm as the characteristic dimension. It is given by

$$Re = 4\rho Q/\pi d\mu \tag{1}$$

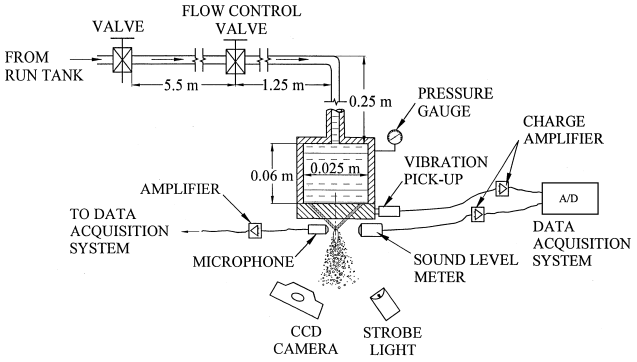

Fig. 3 Schematic of test setup.

The density ρ and viscosity μ were taken to be constant. The Reynolds number in the experiments varied between 5×10^3 and 3×10^4.

The supply pressure to the nozzle was measured using a digital pressure gauge with a resolution 0.002 MPa. The discharge coefficient Cd was defined by the following expression:

$$Cd = Q \Big/ \left[A(2\Delta p/\rho)^{\frac{1}{2}}\right] \tag{2}$$

where A is the cross sectional area of the nozzle and Δp is the pressure drop across the nozzle. The discharge coefficient Cd fell sharply once the flow cavitated. The cavitation parameter was defined following Pearce and Lichtarowicz[15] as

$$\sigma = (p_a - p_v)/(\rho V^2/2) \tag{3}$$

The value of p_a in the preceding expression is the ambient pressure, and p_v is the vapor pressure of the water, which was taken as 0.004 MPa. V is the average flow velocity in the nozzle. The density ρ is taken as constant, and changes in density due to formation of vapor bubbles from cavitation was ignored.

The characteristic frequencies of the disturbances in the spray were determined by sound pressure measurements in the immediate vicinity of the impingement. The disturbances in the liquid spray produce pressure disturbance in the quiescent ambient adjacent to the spray. Capacitance and piezoelectric sensors were mounted in the ambient atmosphere adjacent to the spray in the plane of the impinging jets about 15 mm from the centerline of the spray. The location of the sensors is shown in Fig. 3. The liquid droplets in the spray did not impact on the sensors. The capacitance sensor, which was a miniature collar microphone, had a sensitivity of 3.5 mV/Pa and a flat frequency response upto 20 kHz. The piezoelectric sound level meter had a sensitivity of 0.12 pC/Pa with a resonant frequency of 30 kHz. It was used along with a charge amplifier.

The output from the two transducers were digitized and acquired in a Pentium personal computer using a high-speed data acquisition system at the rate of 10,000 samples per second. LabVIEW software was used for the acquisition and processing of the signals. Data, over a span of 4 s of continuous run of each experiment, were analyzed for the frequency spectrum using the inbuilt fast fourier transform. The frequency spectrum obtained from the microphone and piezoelectric sound pressure level sensor was almost identical, thus, validating the measured frequencies in the spray. A vibration transducer was also mounted on the injector (Fig. 3) to monitor the enhanced vibration due to flow changes in the nozzle. The sizes of droplets formed in the spray were determined using a laser diffraction Malvern particle sizer.

Characteristic Spray Frequencies

Figure 4 is a typical frequency spectrum of the spray obtained at different values of Reynolds number for a nozzle of length-to-diameter ratio of 10. The ordinate is the normalized value of sound pressure level, the normalization being done with reference to the maximum measured sound pressure level. It is observed that pressure amplitudes increase with Reynolds number. However, significant amplitudes are always obtained within about 2000 Hz. Higher

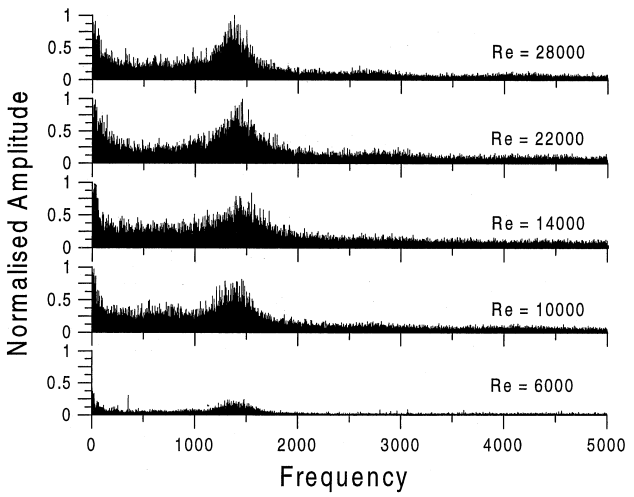

Fig. 4 Frequency spectrum at different Reynolds numbers; nozzle length-to-diameter ratio = 10.

values of pressure amplitudes are seen to be obtained at the lower range of frequencies less than about 150 Hz. The maximum amplitudes are obtained at a frequency of 1450 Hz. All of the nozzles at the different values of Reynolds number gave the peak amplitude at the same value of frequency of about 1450 Hz.

It is necessary to identify the source of the low frequencies less than about 150 Hz and the dominant frequency of about 1450 Hz observed in the spray. Either Kelvin–Helmholtz instability of the liquid sheet formed by the impinging jets could drive the spray frequency or else the individual jets, before the impingement, could have these frequencies (see Refs. 3 and 4). The following correlates the frequencies obtained from different sources with those observed in the spray.

Aerodynamic Instability of the Liquid Sheet

The initial thickness of a liquid sheet formed from the impingement of a pair of liquid jets, is given by Ibrahim and Przekwas[1] as

$$t = \beta r \sin\theta e^{\beta}/(e^{\beta} - 1) \tag{4}$$

where θ is the half-angle of impingement, r is the radius of the jet, and β is a parameter that is determined from the conservation of mass and momentum and is given by

$$\cos\theta = \frac{(e^{\beta} + 1)}{\{(e^{\beta} - 1)[1 + (\pi/\beta)^2]\}} \tag{5}$$

The thickness of the liquid sheet formed by merger of two jets of diameter of 1 mm at an included angle of 75 deg works out to be about 1.2 mm along the axis of the spray. The initial velocity of the liquid sheet can be taken as the jet velocity itself following Ibrahim and Przekwas.[1] With jet velocities in the experiments varying between 3 and 15 m/s, the Weber number of the liquid sheet typically varies between 75 and 1850. The Weber number is defined as

$$We = \rho V^2 (t/2)/\sigma_l \tag{6}$$

where $t/2$ is the half-thickness of the liquid sheet and σ_l is the surface tension coefficient, which for water is 0.073 N/m. The range of frequencies from the aerodynamic instability, calculated from the dispersion relations derived assuming linearized wave motion,[16] gives a frequency of 185 Hz at $We = 75$ increasing to 31,000 Hz at $We = 1850$. The preceding Weber number changes correspond to jet Reynolds number variations between 3×10^3 and 1.5×10^4. Such changes are not seen in the measurements.

Anderson et al.[3] measured the distance separating the wave crests and also the edge ligaments. They also did not find any dependence of the frequencies with changes of the Weber number. Dombrowski

and Hooper,[10] too, did not find any significant influence of the Weber number on the wave motion. Note that the dispersion relation of Squire,[16] used for estimating the frequencies, assumes the flow to be potential and inviscid. Incorporation of viscosity has been shown to slightly reduce the dominant frequencies.[17] The order of magnitude of the predicted aerodynamic frequencies would, therefore, be reasonable. They are nowhere near to the constant values seen in the measurements with changes of Reynolds number.

Dynamics of Feedline and Nozzle

The inertial dynamics in the nozzle and feedline could drive low-frequency oscillations. An estimate of the characteristic of the nozzle and manifold can be made by considering the inertial force in the nozzle and treating the liquid flow to be incompressible.[18] If the pressure drop in a nozzle of length l and cross-sectional area A is Δp_0 for a steady-state flow velocity V_0, the instantaneous pressure drop Δp in the presence of pressure fluctuation at frequency ω can be written as

$$\Delta p = \Delta p_0 + |\Delta p'| e^{i\omega\tau} \tag{7}$$

where $\Delta p'$ denotes the fluctuations in pressure. The pressure drop Δp is from the kinetic and inductive pressure drops, which for ideal flow are given by $\rho V^2/2$ and $\rho l\, \mathrm{d}V/\mathrm{d}\tau$. The inductive pressure drop is obtained from the balance between the acceleration of the volume of liquid in the nozzle, which is balanced by the pressure, namely,

$$\frac{\mathrm{d}}{\mathrm{d}\tau}[(\rho l A)V] = \Delta p_{\mathrm{ind}} A \tag{8}$$

The equation of motion for the flow comprising the kinetic and inertial effects can, therefore, be written as

$$l\frac{\mathrm{d}V}{\mathrm{d}\tau} + \frac{V^2}{2} = \frac{\Delta p}{\rho} \tag{9}$$

If the disturbances in the flow velocity and pressure drop are assumed to be small, we can write

$$V = V_0 + V', \qquad \Delta p = \Delta p_0 + \Delta p' \tag{10}$$

Substituting Eqs. (10) in Eq. (9) and linearizing, we get the flow equation,

$$\frac{\mathrm{d}V'}{\mathrm{d}\tau} + \frac{V_0 V'}{l} = \frac{\Delta p' e^{i\omega\tau}}{\rho l} \tag{11}$$

This gives the velocity disturbance as

$$V' = \frac{\Delta p' e^{i\omega\tau}}{\{\rho l[(V_0/l) + i\omega]\}} \tag{12}$$

$$\frac{V'}{\Delta p'} = \frac{e^{i\omega\tau}}{[\rho V_0(1 + i\omega l/V_0)]} \tag{13}$$

Defining a transfer function Ω given by

$$\Omega = \frac{[V'/V_0]}{[\Delta p'/\Delta p_0]} \tag{14}$$

and substituting in Eq. (13), and simplifying, we get

$$\Omega = \frac{\left\{\Delta p_0 e^{i\omega\tau}[1 - i\omega l/V_0]\right\}}{\rho V_0^2\left[1 + (\omega l/V_0)^2\right]} \tag{15}$$

The ideal pressure drop Δp_0 is equal to $\rho V_0^2/2$ so that the transfer function becomes

$$\Omega = \frac{[1 - i\omega l/V_0]e^{i\omega\tau}}{\left\{2\left[1 + (\omega l/V_0)^2\right]\right\}} \tag{16}$$

The magnitude of the transfer function is, therefore,

$$|\Omega| = 1\Big/\left\{2\left[1 + (\omega l/V_0)^2\right]\right\} \tag{17}$$

This expression shows that the transfer function decreases as frequency increases. This is because the inertia of the liquid is more dominant at the lower frequencies. It is also seen that a decrease in nozzle length l or an increase of injection velocity will lead to increased response.

The upper limit of frequencies ω_u at which the dynamic effects will manifest can be determined as the frequency at which the magnitude of the transfer function becomes 1/e of the maximum. Here e is the logarithmic exponent. The value of ω_u determined from Eq. (17) is given by

$$1\Big/\left[1 + (\omega_u l/V_0)^2\right] = 1/e \tag{18}$$

or

$$\omega_u = (e - 1)^{\frac{1}{2}} V_0/l \tag{19}$$

The liquid jets issuing from short length-to-diameter nozzles would, therefore, contain disturbances over a relatively higher spectrum of frequencies. At higher flow velocities the range of frequencies would likewise increase.

This upper limit of frequencies at which the response is about $1/e$ of the maximum response can be determined from Eq. (19) and works out to be between 30 and 150 Hz as the Reynolds number increases from 5×10^3 to 2.5×10^4. Here the mean length of the nozzle with manifold is taken as 0.06 m (Fig. 3). The frequency spectrum, given in Fig. 4, does indeed show very significant pressure amplitudes at these lower range of frequencies till about 150 Hz. The inertial dynamics of the nozzle and the supply manifold, which drive the low-frequency oscillations, are seen to be reflected in the dynamics of the spray. The frequencies associated with cavitation would also be low considering that the cavitated bubbles are convected at low velocities.[9]

Acoustics of Feed System

The resonant frequencies of the fluid feedline and the nozzle housing could get transmitted to the individual jets and, hence, to the spray. The length of the feedline supplying water to the nozzle after regulation by the needle valve in the experimental setup is 1.5 m (Fig. 3). The frequency of the standing wave mode of oscillations of this feedline considering the valve end and nozzle end as closed is 480 Hz. The speed of sound in water is assumed to be 1500 m/s, and the effective length of the manifold with nozzle is 0.06 m. The characteristic standing wave frequency of the manifold is higher at 12,000 Hz. A closer look at the configuration of flow in Fig. 3 shows a right-angle bend in the feedline after which a length of 25 cm supplies water to the nozzle assembly. If the bend acts as a closed end, the characteristic frequency of this line would be 1500 Hz. This is very near to the observed value of 1450 Hz in the measurements at the peak amplitudes.

Experiments were also done by removing the described bend and an extended 3-m length of flexible hose was used for directly feeding water into the nozzle manifold. The frequency corresponding to maximum sound pressure level reduced to around 300 Hz, thus, suggesting that the dominant frequency in the spray does arise from the characteristic resonant frequencies of the feedline. The low range of frequencies could also be induced from the recirculating flow at entry to the nozzle manifold.

Frequencies from Attachment of Flow in the Nozzle

Frequencies beyond 2000 Hz were not present in the spray obtained from the nozzle of length-to-diameter ratio of 1 at all values of Reynolds number. The flow through the nozzle is detached because the initially separated jet at vena contracta cannot reattach within the short length available (Fig. 2c). The frequency spectrum of the spray issuing from the nozzle of length-to-diameter ratio of 2.3, however, gave significant response at frequencies between 2000 and 5000 Hz for values of Reynolds number of 1.5×10^4 and 2×10^4.

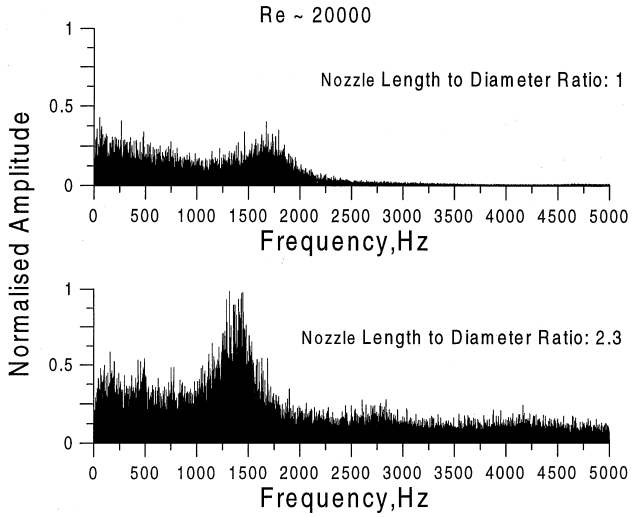

Fig. 5 Changes in frequency spectrum between detached and attached jets.

Figure 5 shows a comparison of the frequency spectrum obtained with nozzles of length-to-diameter ratios of 1 and 2.3 at a Reynolds number of 2×10^4. Though peak amplitudes are present at a frequency of 1450 Hz in both the cases, significant amplitudes are observed for frequencies exceeding 2000 Hz with the nozzle of length-to-diameter ratio of 2.3. The amplitudes at these higher frequencies get sharply reduced when the Reynolds number was further increased to 2.55×10^4 and 2.95×10^4. The insignificant response at the higher values of frequency was qualitatively similar to the results obtained with separated flow in the nozzle of the small length-to-diameter ratio of 1.

At values of Reynolds number exceeding about 2.5×10^4, the cavitation parameter σ is greater than 2.5 and would give rise to supercavitated wall separated flow in the nozzle of length-to-diameter ratio of 2.3. The jet characteristics become similar to the detached jet obtained in the nozzle of length-to-diameter ratio of unity.

The observation, therefore, is that in the presence of attached cavitated flow at Reynolds number of about 2×10^4 ($\sigma \approx 1$), small-pressure amplitudes are present for frequencies exceeding about 2000 Hz and these higher frequencies disturbances disappear for the supercavitated flow. The finding of oscillations present at frequencies exceeding 2000 Hz is also observed with the nozzle of length-to-diameter ratio of 10 for which the flow is always attached. The cavity formed at the vena contracta is unable to penetrate the long length of the nozzle. The attached flow in this nozzle gives rise to higher frequencies of disturbances.

The lower range of frequencies in the spray and the peak amplitudes occurring at frequencies near to the standing wave modes of the feedline suggest that the disturbances in the spray originate in the feedline and are transmitted through the individual jets to the spray.

Configuration of the Spray

Figure 6 shows typical instantaneous photographs of the spray taken in planes along and normal to the plane of the individual jets. The sprays formed from the jets at Reynolds number of 8×10^3, 2×10^4, and 2.8×10^4 are shown. These correspond to cavitation parameters of around 0.3, 1, and 2.8, respectively.

An elliptic-shaped wavy spray, spatially distributed over a wide region but essentially planar, is seen to be formed when the Reynolds number is about 8×10^3. Such two-dimensional sprays normal to the plane of the jets are seen for all nozzles of length-to-diameter ratio between 1 and 10. Intensification of the wave growth over the liquid sheet is observed along the planar sheet, and ligaments are formed and periodically shed. This configuration of the spray is very similar to the laminar and turbulent impinging sprays of Ashgriz et al.[3] and Ryan et al.[4] Though all length-to-diameter ratio nozzles show this wave mode of disintegration at the small values of Reynolds number,

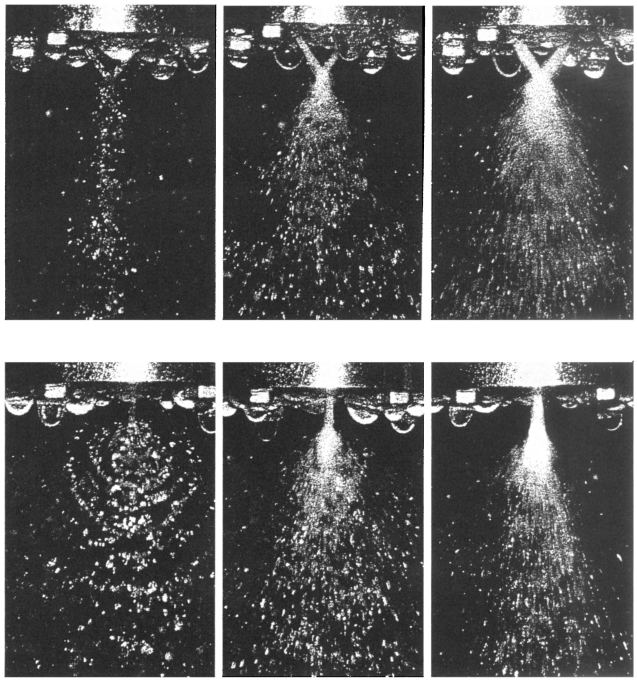

a) $Re \sim 8\times10^3$ b) $Re \sim 2\times10^4$ c) $Re \sim 2.8\times10^4$

Fig. 6 Spray pattern in the plane of the jets and normal to the plane of the jets.

the disturbances and roughness of the liquid sheet are higher for the attached flow obtained with nozzles of length-to-diameter ratio of 3.3 and 10. This is due to the additional disturbances emanating from the attached flow for the longer length-to-diameter ratio nozzle.

When the Reynolds number is increased to a value of about 2×10^4, which corresponds to a cavitation parameter of about unity, a reduction in the width of the spray is observed (Fig. 6). The two jets appear to interact violently by either transmitting into each other or reflecting off each other[2] to form a conical spray unlike the near-planar sprays seen earlier. Droplets are also thrown off during the impact. Divergence of the spray is distinctly observed in the plane of the jets.

These findings are seen to be true for sprays formed by the different nozzles of length-to-diameter ratio between 1 and 10. At a higher values of Reynolds number of about 2.8×10^4 (cavitation parameter $\sigma \approx 2.8$), no traces of waves are seen in the spray. The individual jets, before the impingement, are also seen to be milky white (Fig. 6). The intense turbulent flow gives the milky white appearance to the jets. Ruiz and He[19] discuss on a new species of turbulence generated by cavitation. The impact of these turbulent jets provides a bushy violent structure to the spray. Ryan et al.[4] also observed a shrunk liquid sheet to be formed with a rough and chaotic structure when turbulent jets impinged on each other. The disturbances from cavitation enhance the rough structure leading to the violent conical shape. The changes in the configuration of the spray would influence the droplet sizes, and this is discussed in the next section.

Drop-Size Measurements

Changes in the sizes of droplets formed in the spray due to flow pattern changes are shown in Fig. 7. The Sauter mean diameter D_{32} is measured along the centerline of the spray in the plane of the two jets at a distance 5 cm from the nozzle. At shorter distances, the obscuration was high, resulting in erroneous measurements. For distances greater than 5 cm, the trends of droplet variations with Reynolds number remained the same as obtained at a distance of 5 cm. The variation of D_{32} is plotted as a function of the Reynolds number, cavitation parameter, and Weber number in Fig. 7.

Values of D_{32} are seen to decrease monotonically with increase of Reynolds number when the flow through the nozzle is not cavitated, that is, $\sigma < 1$. The reduction of drop sizes in this noncavitated flow

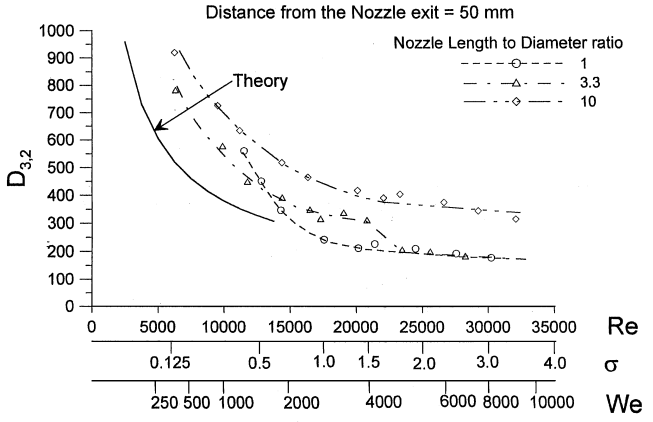

Fig. 7 Droplet size variations for the different nozzles.

regime is in agreement with the theoretical reasoning that an increase of Reynolds number will enhance the shear at the interface of the liquid sheet and the ambient gas and result in the formation of smaller ligaments and droplets. Ryan et al.[4] derive, from linearized wave predictions, the droplet sizes assuming aerodynamic disintegration to be given by

$$D/d = 1.15S^{-\frac{1}{6}}We^{-\frac{1}{3}} \tag{20}$$

where D is the predicted drop size and S is the ratio of gas density to liquid density. The prediction is included in Fig. 7. It is seen that although the predicted values are considerably lower, they show the experimentally observed decreasing trend with increase of Reynolds number till a cavitation coefficient of about unity is reached. Ryan et al.[4] also find the aerodynamic linear instablity theory to predict the trend of droplet size variations reasonably.

Droplets are formed predominantly by aerodynamic disintegration in this zone of small Reynolds number for which the cavitation parameter σ is less than 1. The photograph of the spray in Fig. 6 did show wave buildup and formation of ligaments. This aspect is considered later while discussing the droplet size distributions.

When the flow through the nozzle cavitates ($\sigma > 1$), the measured droplet sizes no longer reduce with the increase of Reynolds number. They tend to remain constant. This is seen in Fig. 7 for all three nozzles for which the results are plotted. The reason for the near-constant sizes for varying Reynolds number could be due to the spontaneous breakup of the liquid jets at impingement from the larger magnitude of the cavitation induced disturbances instead of breakup taking place from intensification of wave motion and thinning of the liquid sheet. The nozzle of length-to-diameter ratio of 3.3 is seen to give droplet sizes of around 300 μm for Reynolds number between 1.8×10^4 and 2.2×10^4. The droplet sizes fall to a value around 200 μm for Reynolds number exceeding about 2.4×10^4. The smaller droplet sizes of 200 μm is the same as obtained for the nozzle with length-to-diameter ratio of unity (Fig. 7). The two distinct values of constant droplet sizes over a range of Reynolds number between 1.8×10^4 and 2.2×10^4 and above 2.4×10^4 are not seen for nozzles of length-to-diameter ratios of 1 and 10. The larger length-to-diameter ratio nozzle is also observed from Fig. 7 to give larger droplet sizes.

The reason for the two steps of droplet sizes for cavitated flow through the nozzle of length-to-diameter ratio of 3.3 and the larger droplet sizes obtained with the nozzle of length-to-diameter ratio of 10 is explained as follows. The cavitation-induced disturbances interact with the nozzle wall on reattachment to give substantial flow disturbances. The larger magnitude of disturbance leads to spontaneous disintegration of a thicker liquid sheet and the formation of larger droplet sizes. For the smaller length-to-diameter ratio nozzle of 3.3, the cavitation bubble can penetrate over the entire length of the nozzle at a cavitation parameter $\sigma \approx 2$, that is, at a Reynolds number of about 2.4×10^4. The flow gets separated from the nozzle walls, and a separated jet, as with the nozzle with length-to-diameter ratio of unity, is obtained. The same sizes of droplets are, therefore, obtained for both these nozzles. However, the cavitated flow for

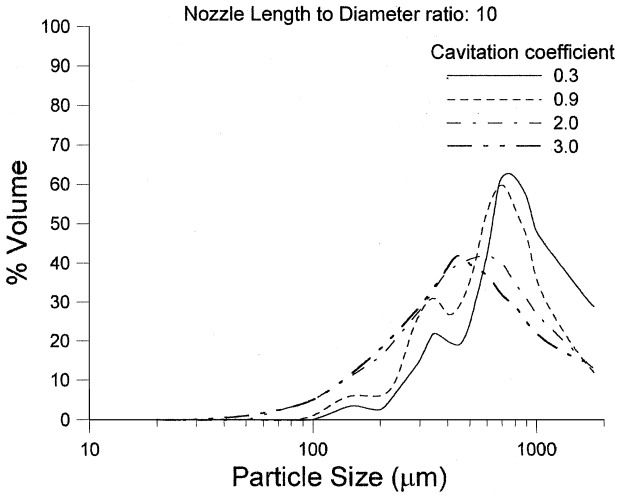

Fig. 8 Changes in the distribution of droplet sizes.

the nozzle of length-to-diameter ratio of 10 is always attached to the nozzle walls and gives larger droplet sizes for $\sigma \gg 1$. The two regions of near-constant droplet sizes obtained with the nozzle of length-to-diameter ratio of 3.3 correspond to cavitated attached flow and cavitated separated flow.

A study of the distribution of the different sizes of droplets in the spray also points toward the absence of the aerodynamic disintegration at the larger values of the cavitation parameter. Figure 8 shows the typical variation of the drop size distribution in the nozzle of length-to-diameter ratio of 10. Such trends were seen for the different length-to-diameter nozzles. A two-peak distribution is obtained at smaller values of Reynolds number for which the flow through the nozzle does not cavitate. A large fraction of droplets has diameter around 800 μm, whereas a smaller fraction is of diameters between 200 and 250 μm when the cavitation parameter $\sigma \approx 0.3$ (Fig. 8). As Reynolds number is increased and cavitation takes place, the peak corresponding the larger diameter droplets is seen in Fig. 8 to shift toward smaller diameters until a distribution with a single peak is obtained for a cavitation coefficient exceeding about 2. It appears that the smaller diameters may arise from impact because they dominate at the larger values of Reynolds number at which aerodynamic disintegration was not seen to be possible and a very bushy turbulent liquid sheet, as shown in Fig. 6, was formed. The dual mode of disintegration transits into a single impact mode of disintegration at the larger values of Reynolds number.

Conclusions

Sprays formed from a pair of attached, separated, and cavitated impinging jets have been evaluated for their characteristic frequencies, shape, and atomization. The wave mode of atomization, observed at the lower range of Reynolds numbers, is shown to transit into either reflective or transmittive atomization with distinctly different behavior when the flow in nozzle cavitates. The length-to-diameter ratio of the nozzle influences the spray characteristics through changed behavior of the flows, which are either attached, detached, cavitated, or supercavitated. The major conclusions of the study are summarized as follows.

1) The dominant frequencies in the spray correspond to the characteristic frequencies of the feed system rather than the wave frequencies from the aerodynamic instability of the liquid sheet formed by the merger of the pair of liquid jets. The frequencies are generally low considering that the dynamics of flow in the feedline and nozzle manifold are driven by the inertial changes. The dominant frequency corresponded to the wave frequency of the supply feedline and remained the same irrespective of the nozzle flow being attached, detached, or cavitated.

2) The configuration of the spray changes from a well-dispersed elliptic shape to an intensively bushy conical shape due to onset of cavitation in the nozzle. The two-dimensional elliptic shape transits to a three dimensional conical configuration. The growth of wave

motion and the formation of ligaments and droplets get arrested. The transmission and reflection of the jets at impingement give a turbulent conical spray instead of an elliptic-shaped wavy spray.

3) The sizes of droplets, formed in the spray, decrease with increase of Reynolds number when the flow through the nozzle is not cavitated. The decrease is in agreement with theoretical predictions obtained by assuming aerodynamic disintegration.

4) The inception of cavitation in the nozzle changes the decreasing trend of droplet sizes with increase of Reynolds number. The droplet sizes no longer change with variations in Reynolds number. However, they are dependent on the nozzle diameter-to-length ratio with the larger length-to-diameter ratio nozzles giving bigger droplets. The disturbances associated with attachment, especially in the presence of cavitation, leads to incipient atomization and the formation of larger droplets in nozzles of increased length-to-diameter ratios. Once supercavitated flow takes place, the droplet sizes become independent of the nozzle length-to-diameter ratio.

5) Dual peaks are obtained in the droplet size distribution at the lower values of Reynolds number due to the two distinctly different processes of aerodynamic disintegration and reflective or transmittive disintegration that are operative at cavitation parameters less than unity. The two peaks merge into a single peak when the flow through the nozzle cavitates, and the aerodynamic disintegration is no longer present.

References

[1]Ibrahim, E. A., and Przekwas, A. J., "Impinging Jet Atomization," *Physics of Fluids A*, Vol. 3, No. 12, 1991, pp. 2981–2987.

[2]Ashgriz, N., Brochlehurst, W., and Talley, D., "Mixing Mechanism in a Pair of Impinging Jets," *Journal of Propulsion and Power*, Vol. 17, No. 3, 2001, pp. 736–749.

[3]Anderson, W., Berthoumieu, P., Huang, C., Lecount, R., Yatsuyanagi, N., and Zhu, N., "Atomization of Impinging Liquid Jets," *Proceedings of the 2nd International Symposium on Liquid Rocket Propulsion*, ONERA, 1995, pp. 3.1–3.19.

[4]Ryan, H. M., Anderson, W. E., Pal, S., and Santoro, R. J., "Atomization Characteristics of Impinging Liquid Jets," *Journal of Propulsion and Power*, Vol. 11, No. 1, 1995, pp. 135–145.

[5]Nurick, N. H., "Orifice Cavitation and its Effect on Spray Mixing," *Journal of Fluids Engineering*, Vol. 98, Dec. 1976, pp. 681–687.

[6]Tamaki, N., Schimuzu, M., Nishida, K., and Horoyasu, H., "Enhancement of Atomization of a Liquid Jet by Cavitation in a Nozzle Hole," *Atomization and Sprays*, Vol. 11, No. 2, 2001, pp. 125–137.

[7]Heidmann, M. F., Priem, R. J., and Humphrey, J. C., "A Study of Sprays Formed by Two Impinging Jets," NACA TN 3835, March 1957.

[8]Karasawa, T., Tanaka, M., Abe, K., and Kurabayashi, T., "Effect of Nozzle Configuration on Atomization of a Steady Spray," *Atomization and Sprays*, Vol. 2, No. 4, 1992, pp. 411–426.

[9]Henry, M. E., and Collicotte, S. H., "Visualization of Internal Flow in a Cavitating Slot Orifice," *Atomization and Sprays*, Vol. 10, No. 6, 2000, pp. 545–563.

[10]Dombrowski, N., and Hooper, P. C., "A Study of the Sprays Formed by Impinging Jets in Laminar and Turbulent Flow," *Journal of Fluid Mechanics*, Vol. 18, Pt. 3, 1963, pp. 392–400.

[11]Wang, G., Senocak, I., Shyy, W., Ikohagi, T., and Cao, S., "Dynamics of Attached Turbulent Cavitating Flow," *Progress in Aerospace Science*, Vol. 37, No. 5, 2001, pp. 551–581.

[12]Williams, F. A., "Steady State Processes," *Liquid Propellant Rocket Combustion Instability*, edited by D. T. Harrje and F. H. Reardon, SP-194 NASA, 1972, pp. 46–49.

[13]Ramamurthi, K., Nandakumar, K., Shankar, S., and Patnaik, R., "Hysteresis and Bifurcation of Flow in Fuel Injection Nozzles," *Journal of Aerospace Engineering*, Vol. 215, No. 1, 2001, pp. 49–59.

[14]Ramamurthi, K., Nandakumar, K., and Patnaik, R., "Two Step Start Transients with Long Feedlines Discharging Liquid Through Sharp-edged Cylindrical Nozzles," *Atomization and Sprays*, Vol. 12, No. 1–3, 2002, pp. 193–207.

[15]Pearce, I. D., and Lichtarowicz, A., "Discharge Coefficient of Long Orifice with Cavitating Flow," *Proceedings of the Second Fluid Power Symposium*, Jan. 1971, pp. D2.13–D2.35.

[16]Squire, H. B., "Investigations of Instability of Moving Liquid Film," *British Journal of Applied Physics*, Vol. 4, No. 6, 1953, pp. 167–169.

[17]Cousin, J., and Dumouchel C., "Effect of Viscosity on the Linear Instability of a Flat Liquid Sheet," *Atomization and Sprays*, Vol. 6, No. 5, 1996, pp. 563–576.

[18]Bazarov, V. G., *Dynamics of Liquid Injectors*, Mashinostroyenie, Moscow, 1979 (in Russian), pp. 11, 12.

[19]Ruiz, F., and He, L., "Turbulence Under Quasi-steady Conditions: A New Species," *Atomization and Sprays*, Vol. 9, No. 4, 1999, pp. 419–429.